Validity of the rigid band approximation in the study of the thermopower of narrow band gap semiconductors

Mal-Soon Lee and S. D. Mahanti

Phys. Rev. B **85**, 165149 — Published 30 April 2012

DOI: 10.1103/PhysRevB.85.165149

Validity of the rigid band approximation in the study of thermopower of narrow band gap semiconductors

Mal-Soon Lee and S. D. Mahanti
Department of Physics and Astronomy, Michigan State University, East Lansing, MI 48824
(Dated: April 17, 2012)

Theoretical studies of thermoelectric properties using *ab initio* electronic structure calculations help not only to understand existing experimental data but also to predict new materials which can be potentially good thermoelectrics. However, in these studies it is inevitable to employ some approximations. It is therefore important to verify their reliability. To this end, we have investigated the validity of the rigid band approximation (RBA), commonly used in calculating thermopower (S) in doped (sometimes heavily) narrow band gap semiconductors. We have considered two important systems: half-Heusler (HH) HfCoSb and PbTe. We calculate band structures of pure and doped systems (using quasi-periodic approximation-QPA) by employing density-functional method. We then use Boltzmann transport theory to calculate thermopower using both RBA and the band structure with QPA. We find that band structures do not change significantly when isovalent impurities are present excepting in specific cases. However, charged impurities (relevant to the doping case) providing carriers can change the host band structure appreciably. We find that impurities in general remove existing degeneracies which tend to reduce the RBA value of $\mid S \mid$. The reduction is significant in both HfCoSb and PbTe when charged defects are present.

PACS numbers: 71.15.Mb, 71.55.-i, 72.10.-d, 84.60.Rb

I. INTRODUCTION

Thermoelectric (TE) devices are used for energy conversion such as power generation from waste heat or heat pumps for heating or cooling. The efficiency of thermoelectrics depends on the transport coefficients of a TE material through the dimensionless figure of merit $ZT = S^2\sigma T/\kappa$, where σ is the electrical conductivity, S is the thermopower (or Seebeck coefficient), T is temperature, and κ is the thermal conductivity. The thermal conductivity is given by the sum of contributions from the electronic carriers (κ_{el}) and the lattice (κ_l). To improve the efficiency of thermoelectrics (which depends on ZT), one can use two different approaches : increase the power factor ($PF = S^2\sigma$) which is usually achieved by engineering the electronic structure, and reduce κ by introducing phonon scatterers without affecting the electron transport.[1,2] However, the fact that increasing σ by increasing the carrier concentration usually decreases the magnitude of S and increases κ_{el} makes the first approach rather difficult.

Metals have large σ but very small $\mid S \mid$ whereas insulators have very small σ but large $\mid S \mid$. Both these are not good thermoelectrics. On the other hand, narrow-band-gap semiconductors optimize both σ and $\mid S \mid$ and are known to be best thermoelectrics. Also, in semiconductors one can control the transport properties by carefully controlling the carrier concentration through doping. In fact, it is well known that changes in the carrier concentration and manipulation of the electronic structure in the neighborhood of the band gap and chemical potential can indeed increase the power factor of the material.[3] For example, Heremans *et al.* doped Tl impurities in PbTe which is known to create a resonance state near the top of the valence band and change the host band structure.[4] Similarly Androulakis *et al.* use K defects to produce strain induced changes in the band structure while controlling the carrier concentration though Na impurities.[5]

From a theoretical prospective, thermoelectric properties are obtained by first carrying out electronic structure calculations using *ab initio* methods and then using these results in transport coefficient calculations. Theoretical calculations are used not only to understand the existing experimental results but also to predict potentially new high performance thermoelectric materials. In carrying out these calculations one usually makes several approximations, one of them is the RBA. In RBA, it is assumed that the band structure of the host is unchanged by doping. However, its validity needs to be carefully checked. This is the main focus of this work. For the sake of illustration we have chosen two very well studied systems: one HH compound HfCoSb, and the other PbTe.

HfCoSb crystallizes in the cubic MgAgAs-type structure which can be regarded as four interpenetrating face-centered cubic (FCC) lattices: a lattice of Hf atoms and a lattice of Sb atoms, together forming a rock-salt structure, and a lattice of Co atoms occupying the center of every other Hf_4Sb_4 cube formed by nearest neighbor Hf and Sb atoms, while the centers of the remaining Hf_4Sb_4 cubes are vacant.[6] Half-Heuslser compounds are semiconductors when there are 18 valence electrons per unit cell.[7–12] This is indeed seen in HfCoSb where calculations with local density and generalized gradient approximations (LDA/GGA) give a band gap of $\sim$1.0 eV at 0 K. Compared to HfCoSb, PbTe has a simple rocksalt structure with 2-interpenetrating FCC lattice. The band structure of PbTe is well-known.[13] GGA calculations give a direct band gap of 0.2 eV (at 0 K) where the valence band maximum and the conduction band minimum occur at the L point of the Brillouin Zone (BZ). When optimally doped, both HfCoSb and PbTe give relatively high power factors at mid-temperature range (300 K$\leq T \leq$ 800 K). This has made them quite attractive for thermoelectric devices.[14–19]

Theoretical electronic structure calculations give the band structures $\varepsilon_{i,\mathbf{k}}$, where i is the band index and $\mathbf{k}$ is the wave vector of the electron. Using these $\varepsilon_{i,\mathbf{k}}$ one calculates transport coefficients. Within Boltzmann transport equation approach, tensors of electrical conductivity ($\sigma_{\alpha\beta}$) and Seebeck coefficient ($S_{\alpha\beta}$) at zero electric field $\mathbf{E}$ are given by

$$\sigma_{\alpha\beta}(T,\mu) = \frac{1}{\Omega}\int \sigma_{\alpha\beta}(\varepsilon)\left[-\frac{\partial f_0(T,\varepsilon,\mu)}{\partial\varepsilon}\right]d\varepsilon, \tag{1}$$

$$\nu_{\alpha\beta}(T,\mu) = \frac{1}{eT\Omega}\int \sigma_{\alpha\beta}(\varepsilon)(\varepsilon-\mu)\left[-\frac{\partial f_0(T,\varepsilon,\mu)}{\partial\varepsilon}\right]d\varepsilon, \tag{2}$$

$$S_{ij} = (\sigma^{-1})_{\alpha i}\nu_{\alpha j}, \tag{3}$$

where e is the electronic charge, α and β are tensor indices, Ω, μ, and f_0 are the volume of unit cell, chemical potential, and Fermi-Dirac distribution function, respectively. In Eqn. 3, repeated index α implies summation over that index. In Eqs. 1 and 2, the transport function (TF) tensor $\sigma_{\alpha\beta}(\varepsilon)$ is defined as

$$\sigma_{\alpha\beta}(\varepsilon) = \frac{e^2}{N}\sum_{i,\mathbf{k}}\tau(i,\mathbf{k})\cdot\upsilon_\alpha(i,\mathbf{k})\cdot\upsilon_\beta(i,\mathbf{k})\cdot\delta(\varepsilon-\varepsilon_{i,\mathbf{k}}), \tag{4}$$

where N is the number of $\mathbf{k}$ points sampled in the 1$^{\text{st}}$ Brillouin zone (BZ) in the $\mathbf{k}$-summation. In the TF tensor, $\upsilon_\alpha(i,\mathbf{k})(\alpha = x,y,z)$ is the α^{th} component of the group velocity $\mathbf{v}(i,\mathbf{k})$ of carriers and $\tau(i,\mathbf{k})$ is the relaxation time. The velocities can be obtained from the band dispersion using the relation

$$\upsilon_\alpha(i,\mathbf{k}) = \frac{1}{\hbar}\frac{\partial\varepsilon_{i,\mathbf{k}}}{\partial k_\alpha}. \tag{5}$$

As shown above, thermopower and electrical conductivity are functions of the TF, which is energy dependent, coming from the density of state (DOS), velocity of carriers $\mathbf{v}(i, \mathbf{k})$, and relaxation time $\tau(i,\mathbf{k})$. Among these, DOS and $\mathbf{v}$ are directly affected by the electronic structure, $\varepsilon_{i,\mathbf{k}}$.

In theoretical calculations of transport coefficients, particularly in complex systems, one commonly uses two approximations: rigid band approximation (RBA) and energy-independent relaxation time. In RBA it is assumed that doping a system does not change the host band structure, only the chemical potential changes with doping concentration and of course temperature. The relaxation time in general depends on energy (ε) and temperature (T) i.e. $\tau(\varepsilon,T)$. The T dependence of transport coefficients such as σ, S, and κ_{el} comes from, in addition to other sources, explicit T dependence of $\tau(\varepsilon,T)$ and implicitly through its energy dependence. A full energy and T dependence study of $\tau(\varepsilon,T)$ using *ab initio* band structure calculations even in simple semiconductors is not possible at the present time. However, detailed studies of $\tau(\varepsilon,T)$ using Kane model band structures and theoretical expressions developed by Ravich *et al.*[20,21] for electron-impurity and electron-phonon couplings have been done in PbTe[22,23] and Bi_2Te_3.[24] Ahmad and Mahanti[23] found that the total relaxation time in PbTe can be approximated extremely well by a scaling equation

$$\tau_{tot}(\varepsilon,T) = \frac{aT^{-p}}{b + c\varepsilon^{r}}, \tag{6}$$

where the parameters a, b, c, p and r are T and ε independent but depend on carrier concentration and other fundamental constants such as electron-phonon coupling strength, etc. They found that the energy dependence, controlled by the parameter r had very little contribution to the T dependence of the transport coefficients, the major contributions coming from the parameter p and the T dependence of other parameters such as band gap, effective mass, etc. In particular, in the calculation of thermopower where $\tau(\varepsilon,T)$ appears both in the numerator and denominator, the major T-dependent factor cancels out keeping only the weak r-dependent term. Since the T-dependence of σ was hardly affected by r (see Fig. 10 of ref 23), we can assume $\tau(\varepsilon,T)$ to be energy independent in the calculation of transport coefficients at temperatures where electron-phonon scattering (from both acoustic and optical phonons) control the relaxation time. In this paper, therefore, we have assumed $\tau(\varepsilon,T)$=$\tau(T)$. In this way, we decouple the two major approximations, study each of them separately. Also, Chaput *et al.* have calculated S using a simple model which takes into account the k-dependence of τ in doped skutterudites.[25] They also find a rather small difference in the S from constant τ approximation.

Recently Popescu and Woods (PW) have discussed the possibility of enhancing thermoelectric properties (power factor-PF and ZT) of PbTe by electronic structure modifications and nanostructuring.[26] For the former they use a modified density of states caused by a resonant state (due to an impurity) near the chemical potential. With this modified DOS and the associated transport velocity they have calculated the PF using energy-dependent relaxation time.[22] For the same carrier concentration, they indeed find an enhancement in the PF (and also ZT) depending on the position and width of the resonance peak. This indicates that RBA is not adequate for impurities (dopants) which strongly modify the host DOS. Although the PW model is empirical, this is an exciting result. To see if such an enhancement will be present in more realistic electronic structure calculations and to critically test the validity of RBA, we have investigated the effect of impurity on the electronic structure and transport properties by employing *ab initio* calculations. For this purpose we investigate the electronic structure and thermopower of PbTe and HfCoSb with different concentrations and types of impurities.

The paper is arranged as follows. In Sec. II, we briefly describe the computational procedure. We present our results and discussion in Sec. III. A brief summary is given in Sec. IV.

II. COMPUTATIONAL DETAILS

Scalar relativistic electronic structure calculations were carried out within density-functional theory (DFT) using the projector augmented wave (PAW) methods[27] as implemented in VASP.[28] The Perdew-Burke-Ernzerhof (PBE) generalized gradient corrected exchange-correlation functionals[29] were used in our calculation. An energy cutoff of 400 eV was used for the plane-wave expansion, with a total energy convergence of the order of 10^{-4} eV.

We use the quasi-periodic approximation (QPA) to calculate the effect of impurity on the band structure. In this model the impurities are introduced into a periodic array of supercells of the host. If the size of the supercell is large enough, then the interaction between the impurities belonging to different supercells is negligible.

We first start our calculations with the FCC primitive unit cell having three atoms Hf, Co, and Sb in HfCoSb, and two atoms Pb and Te in PbTe. We then calculate the band structure of the pure compounds using a simple cubic (SC) unit cell ($1\times1\times1$) having 12 atoms for HfCoSb, and a $2\times2\times2$ cubic supercell (CSC) having 96/64 atoms for HfCoSb/PbTe. We introduce impurities in the $1\times1\times1$ SC and/or $2\times2\times2$ CSC. We optimized the lattice parameters as well as the ionic positions using total energy calculations for all the cases studied. These optimized structures are then used to calculate the electronic band structure and other properties. For PbTe, we include spin-orbit interaction (SOI) since it is known to be very important.[30] However, SOI effect is found to be negligible in HfCoSb.

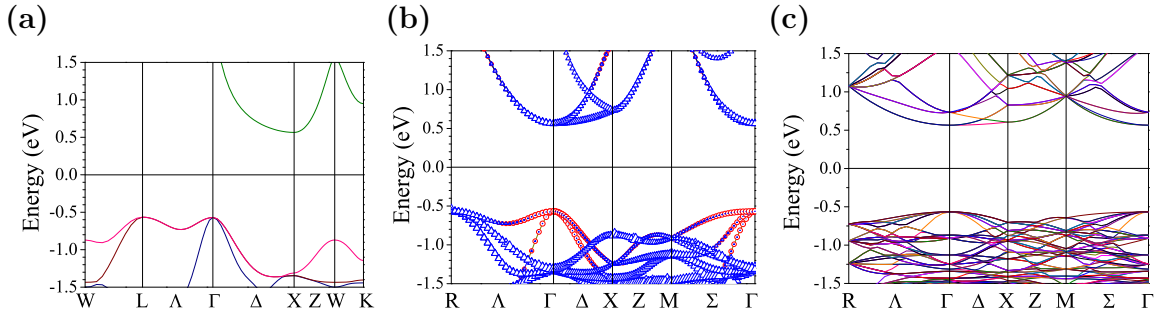

FIG. 1. Band structure of HfCoSb with different BZ schemes: (a) FCC, (b) simple cubic (SC), and (c) $2\times2\times2$ cubic supercell (CSC). For SC, we show the contribution of Co *d* orbital (blue triangles) and Hf *d* orbital (red circle) to the bands. The size of the symbols represents the strength of the contributions. The Fermi level is set to be at zero energy.

An accurate study of defect induced changes in the band structure requires large supercells. Similarly accurate calculation of transport coefficients requires a dense sampling of the **k**-space. In addition to these, if SOI interaction is important and one has to include SOI in the band structure and transport coefficient calculations, the computational requirement becomes extremely prohibitive. We have therefore calculated thermopower for HfCoSb and PbTe without SOI. This should be adequate for HfCoSb. We will show that this is also adequate for PbTe.

Thermopower of HfCoSb with and without impurity were calculated using band structure obtained with $31\times31\times31$ Monkhorst-Pack **k**-point samplings[31] for $(1\times1\times1)$ SC to get more accurate velocities.[22,25,32–35] In case of PbTe, $21\times21\times21$ **k**-point sampling was used for the CSC. The transport coefficients were calculated using BoltzTrap developed by Madsen and Singh (MS).[33] Note that for accurate calculations of transport coefficients one needs to use very large number of points in the summation over **k** (See Eqn. 4). MS have employed an interpolation method to obtain accurate values for $\mathbf{v}(i,\mathbf{k})$ by fitting the band structure to analytical forms using a dense **k** mesh.

III. RESULTS AND DISCUSSION

A. HfCoSb

1. *Band structure*

As discussed earlier, HfCoSb consists of four inter-penetrating FCC sublattices: Hf at (0, 0, 0); Co at $(\frac{1}{4},\frac{1}{4},\frac{1}{4})$; Sb at $(\frac{1}{2},\frac{1}{2},\frac{1}{2})$ and vacancy at $(\frac{3}{4},\frac{3}{4},\frac{3}{4})$. The band structure in the FCC BZ along symmetry directions $W-L-\Gamma-X-Z-W-K$ near the Fermi level is shown in Fig. 1(a). It shows an indirect gap of 1.13 eV. The valence band maximum (VBM) occurs at the *L* point and is nearly degenerate (within $\sim$4 meV) with the maximum at the Γ point. The conduction band minimum (CBM) occurs at the *X* point. There are two degenerate bands at the L point and three degenerate bands at the Γ point for the VBM. However, there is no degeneracy for the CBM.

To study impurity effects in a system using the QPA, one first needs to understand how the band structure of the pure HfCoSb looks like with different types of BZ such as FCC, $(1\times1\times1)$ SC, and $2\times2\times2$ CSC.[36] We show the band structure with SC cell along high-symmetry directions $R-\Gamma-X-M-\Gamma$ in Fig. 1(b). The VBM occurs at the *R* point, and nearly degenerate with the one at the Γ point. The CBM occurs at the Γ point. Let us first understand the difference in the band structures between FCC and SC BZ's. The volume of SC BZ is $\frac{1}{4^{\text{th}}}$ of the FCC BZ and SC BZ maps inside the FCC BZ. The *L* point in the FCC BZ maps to the *R* point in the SC BZ. In addition, folding at the middle of Γ-*X* in the FCC BZ corresponds to Γ-*X* in the SC BZ. Thus the middle point of Γ-*X* in the FCC BZ becomes the *X* point in the SC BZ. Because of this mapping, the position of the VBM changes from the *L*-point in the FCC BZ to the *R*-point in the SC BZ, and the CBM which is at the *X*-point in the FCC BZ maps to the Γ point in the SC BZ. When we use CSC BZ (Fig. 1(c)), each symmetry direction between Γ and *R*/*X*/*M* of the SC BZ is folded through the middle. Thus, *R*-, *X*-, and *M*-points in the SC map to the Γ-point in the CSC BZ. This results in the VBM to be at the Γ point. One can see that the band structure maps and agrees very well not only for the overall shape but also for the detail energy values when the bands are folded from FCC to CSC via SC BZ's. This gives us confidence in the convergence of the $2\times2\times2$ supercell calculations.

In our previous paper[37] we have pointed out that the calculated transport properties in HfCoSb with RBA gives the highest power factor (PF) for a hole concentration of $\sim4\times10^{21}/\text{cm}^3$ corresponding to a doping of 25 %, assuming that each dopant contributes one hole. The fundamental question we address here is whether for such a large concentration of holes *i.e.* doping level, is RBA good? To answer this question, we use a SC cell with 4 atoms of each element and replace one of the elements

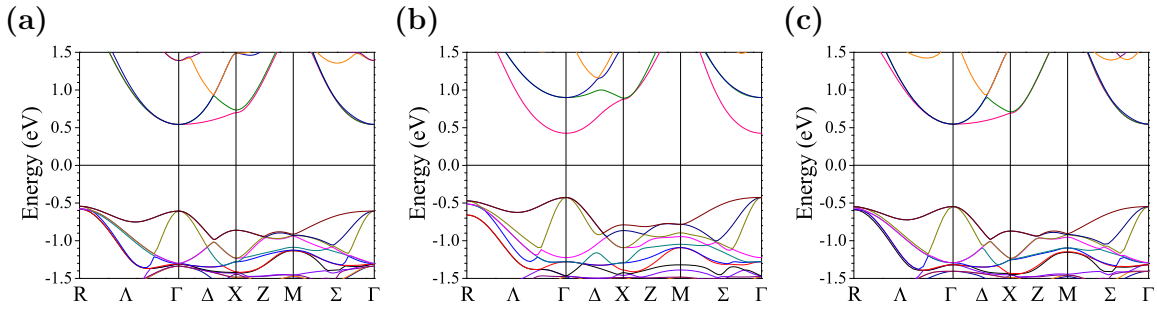

FIG. 2. Band structure with SC BZ for (a) $Hf_{0.75}Zr_{0.25}CoSb$, (b) $HfCo_{0.75}Ir_{0.25}Sb$, (c) $HfCoSb_{0.75}Bi_{0.25}$. The Fermi level is set to be at zero energy.

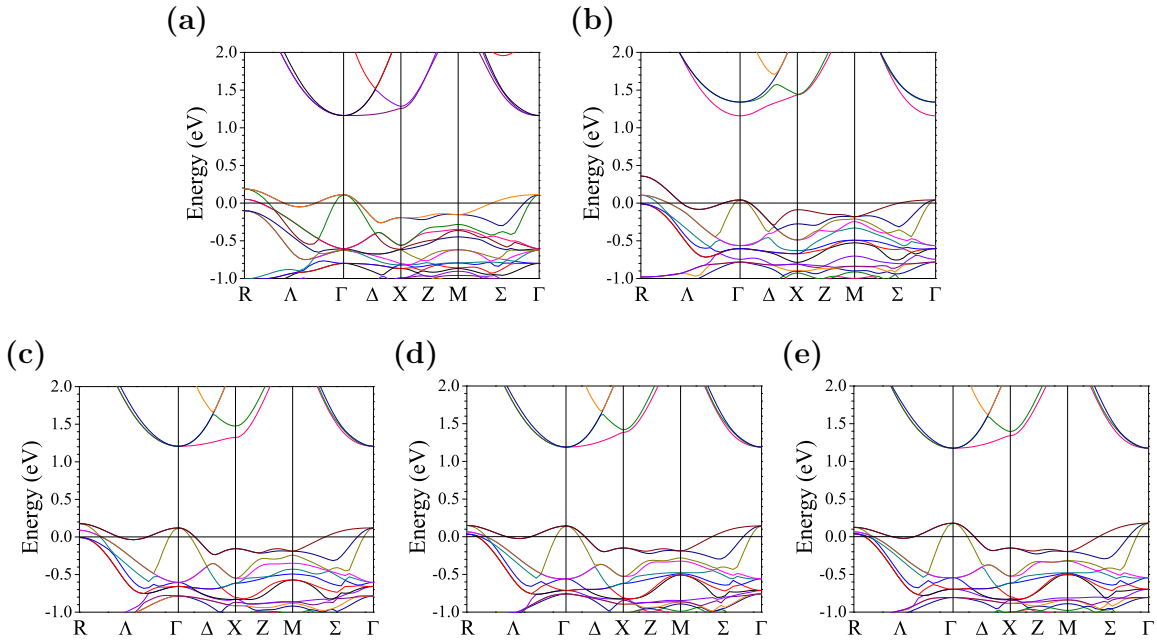

FIG. 3. Band structure with SC BZ for (a) $Hf_{0.75}Y_{0.25}CoSb$, (b) $HfCo_{0.75}Fe_{0.25}Sb$, (c) $HfCoSb_{0.75}Ge_{0.25}$, (d) $HfCoSb_{0.75}Sn_{0.25}$, (e) $HfCoSb_{0.75}Pb_{0.25}$. The Fermi level is set to be at zero energy.

by an impurity atom, resulting in 25 % doping. We study both isovalent-impurities and impurities that lead to *p*-doping. We show the band structure of isovalent impurities in Fig. 2, where the impurities and the atom they replace are (a) Zr, Hf (b) Ir, Co and (c) Bi, Sb. These should be compared with Fig. 1(b), where we plot the contribution from *d*-orbitals of Co and Hf. As seen in Fig. 1(b), VBM at the *R* point and CBM at the Γ point are predominantly Co-*d*, while VBM at the Γ point is Hf-*d*. Ir substitution changes the host band structure significantly for both VBM near the *R*-point and CBM near the Γ-point (compare Figs. 1(b) and 2(b)), while Zr or Bi substitution does not change the host band structure appreciably (compare Figs. 1(b) and 2(a), 2(c)). Interestingly, in contrast to the VBM at the R point, the one at the Γ-point is not affected by the impurities.

As regards *p*-doping impurities we replace (i) Hf by Y, (ii) Co by Fe, (iii) Sb by Ge/Sn/Pb, and the corresponding band structures are shown in Fig. 3. In contrast to the isovalent impurities, *p*-doping impurities distort the host band structure considerably in all cases. Similar to the isovalent impurities, the largest change is again seen for Fe-substitution at the Co-site, but the change in the valence bands is more than that in the conduction bands. However, when Sb is replaced by an impurity atom, the change is small compared to the substitution at the transition metal sites Hf and Co. The smallest change is seen in the case of Sn substitution. For both isovalent and *p*-doping impurities, the largest change occurs at the *R*-point where the degeneracy is removed. Interestingly, conduction bands near the Fermi level are not affected much by the impurities except when the Co site is involved, because CBM is primarily of Co-*d* states. Also the VBM at the Γ-point is not perturbed by the impurities, similar to what we found for the isovalent impurities.

Since the above doping levels are quite large, the effect of impurities on the band structure is expected to be quite large. In experiments one deals with lower doping levels. To see what happens to the band structures for lower doping levels, we have used a $2 \times 2 \times 2$ cubic supercell which contains 32 atoms of each element of the host, and replace 1, 4, and 8 Sb atom(s) with

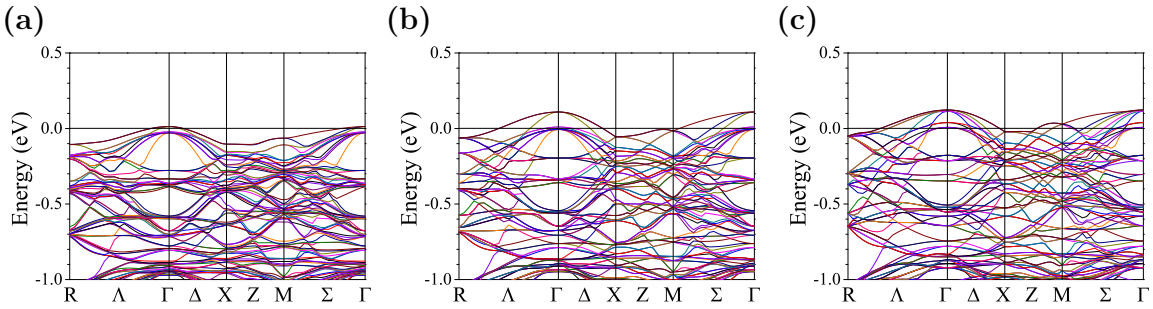

FIG. 4. Band structure using $2 \times 2 \times 2$ CSC BZ for $HfCoSb_{1-x}Sn_x$ with (a) x=0.03125, (b) x=0.125, and (c) x=0.25. The Fermi level is set to be at zero energy.

Sn, corresponding to 3.125, 12.5, and 25.0 % of doping, respectively. To check the structural preference, we have calculated the total energy of segregation and non-segregation cases for 12.5 % doping. We find that Sn impurities prefer to segregate, and have therefore used a structure with segregated Sn atoms for 4 and 8 Sn-doping cases to calculate the band structure. As seen in Fig. 4 which should be compared with Fig. 1(c), even with 3.125 % doping, the valence band structure shows the removal of degeneracies at Γ- and *R*-points and the size of splitting increases with increasing doping level.

2. Thermopower

We have calculated thermopower of different systems with impurities as well as pure HfCoSb as a function of temperature (Fig. 5). For pure HfCoSb and the isovalent impurity systems, we use the RBA and consider one hole per unit cell which corresponds to a 25 % doping level. This is the same doping level as the non-isovalent cases. Let's first discuss the isovalent impurity cases shown in Fig. 5(a). *S* for (Hf,Zr)CoSb and HfCo(Sb,Bi) are very close to that for HfCoSb, consistent with small changes in the band structures of HfCoSb with impurities at the Hf and Sb sites. For Hf(Co,Ir)Sb, *S* values are reduced by $\sim 10-20$ %, due to the removal of degeneracy at the *R* point in the band structure (Fig. 2(b)). For the *p*-doped systems (Fig. 5(b)), we have calculated *S* using the perturbed band structures and compared with that obtained in RBA. The *S* values calculated using the perturbed band structures tend to be smaller than that obtained with RBA. Larger the change in the band structure, larger the decrease in thermopower. The smallest thermopower (about 20 % reduction from RBA value at 1000 K) is obtained in Fe-doped system which shows the largest perturbation of the host band structure. In our previous paper,[37] we have discussed how contribution from different carrier pockets affects the value of *S*. It is also known that *S* depends on the degeneracy and number of symmetry points in the BZ in addition to the effective mass. Thus, relative contribution from Γ and *R* pockets affects *S* value. Because of this, the smallest *S* found for the Fe-doped system is due to contributions mainly from small effective mass carriers with removed degeneracy near the top-most valence band at the *R* point (originally the *L* pockets in the FCC BZ) and a small contribution from the Γ pocket where the degeneracy is preserved. In contrast to the above, when Sb is replaced by Sn or Ge, the band structures show that nearly similar contributions to *S* come from both *R* and Γ pockets. In addition, there is no significant change in the effective mass in spite of the removal of degeneracy at the *R* point. We note that the reduction of the gap does not affect thermopower and its *T*-dependence since the gap is already large ($\sim$1.0 eV) and there is very little contribution from electron-hole excitations which tend to reduce the value of $\mid S \mid$. We find that the reduction in *S* from its RBA value is smallest for Sn and Ge among the *p*-doped systems. Slightly larger reduction of *S* in the case of Pb substitution is perhaps due to different relative contributions from the Γ and *R* pockets compared to Sn and Ge.

It is well known that a major drawback of half-Heusler compounds for TE applications is their high thermal conductivity. Thus to improve their TE performance, scattering centers are introduced by putting impurities. For this purpose, one usually replaces Hf by Zr in HfCoSb. Based on our calculations, replacement of Sb by Bi impurity does not reduce thermopower. We, therefore, suggest that in addition to HF/Zr mixing, Sb and Bi mixing and doping with Sn and Ge will further reduce the thermal conductivity without degrading the thermopower. Thus, we believe that the calculation of the band structure with impurity and comparison with host band structure can be used as a reliable guide for not only the optimum doping level but also for the type of impurity one should use to improve TE performance.

B. PbTe

PbTe is a well-known narrow band gap semiconductor. The calculated band structure with FCC unit cell using the optimized lattice constant (a=6.557 Å) is shown in Fig. 6(a). It gives a direct band gap at the *L* point. The second highest valence band

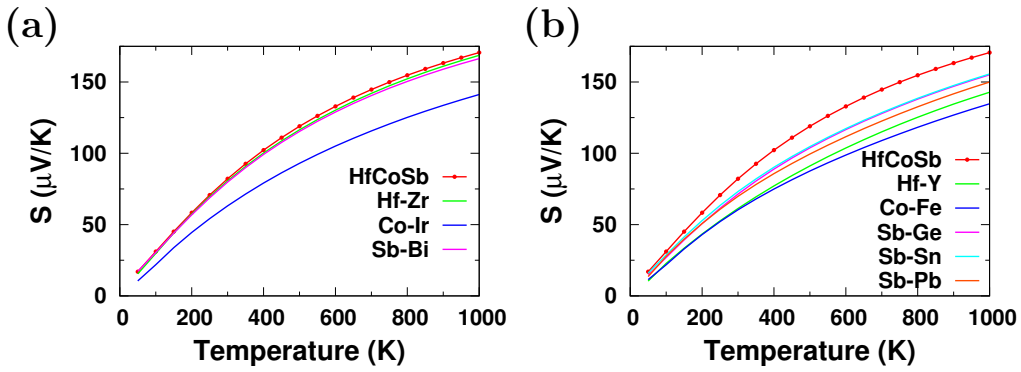

FIG. 5. Calculated thermopower of (a) isovalent impurity, (b) *p*-doping along with that of pure HfCoSb as a function of temperature. Thermopower of pure and isovalent-impurity HfCoSb is obtained using RBA. The corresponding carrier concentration is $4.5 \times 10^{21}/\text{cm}^3$.

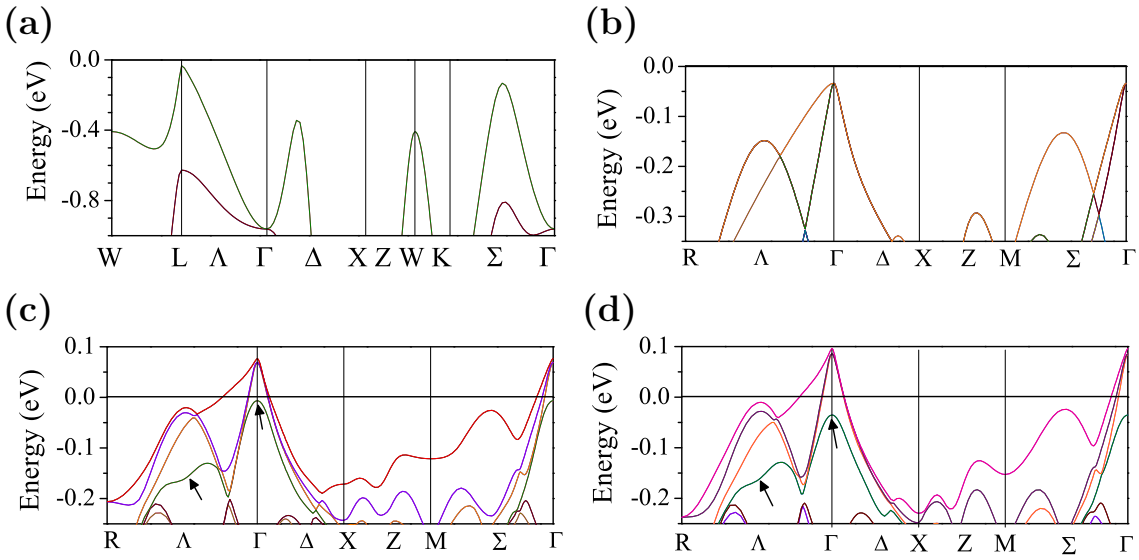

FIG. 6. Band structure of (a) PbTe with FCC BZ, (b) PbTe with CSC BZ, (c) K-doped PbTe with CSC BZ, and (d) Na-doped PbTe with CSC BZ. the Fermi level is set to be at zero energy.

maximum occurs at a point joining Γ and *K* which we will loosely refer as the Σ point and its energy is only 0.1 eV lower compared to the energy at the *L* point. This is important for transport since carriers around Σ can be introduced with rather small doping levels. In order to check the validity of RBA when K/Na impurities are introduced, we have calculated the band structure of undoped PbTe using a $2 \times 2 \times 2$ supercell as shown in Fig. 6(b). We omit here the comparison between different BZ's since it has been discussed by Hoang and Mahanti (see Ref. 38) and also in Sec. III A for HfCoSb. We only point out the difference in the band structures between the FCC and CSC BZ's. In addition to the second valence band maximum at Σ seen in the band structure with the FCC BZ, the band structure of the CSC-BZ shows a third valence band maximum near the middle of the line joining Γ and *R*, *i.e.* along the Λ direction. Its energy is ∼0.02 eV lower than the Σ point maximum. This implies that the energy landscape of PbTe is more complex compared to what is seen in the band structure shown along the symmetry directions of the FCC BZ.

Recently Androulakis *et al.* studied K and/or Na doped PbTe with varying doping levels upto 2.5 %.[5] They found that the thermopower becomes nearly constant for hole concentrations $n \geq 4 \times 10^{19}/\text{cm}^3$. They explained this observation with two valence band maximum model. Motivated by their studies, we calculate the band structures of K- or Na-doped PbTe. Starting from $2 \times 2 \times 2$ supercell of PbTe we replace one Pb with either a K or a Na, which corresponds to 3.125 % doping. The optimized lattice constants are 13.134 Å with K-doping and 13.102 Å with Na-doping, while it is 13.114 Å for pure PbTe. This tendency has been observed by Adroulakis *et al.* although the changes in the lattice constant seen in the experiments are smaller than ours. They suggest that an increase of the lattice constant by putting K in PbTe results in a decrease of the energy difference between the two valence band maxima occurring at *L* and Σ, which can in turn affect their transport properties. We will address this question in a future paper. For the present, we will confine to the issues of RBA.

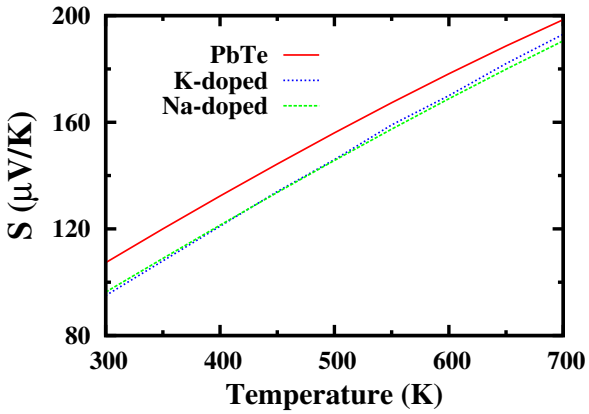

FIG. 7. Comparison of thermopower with and without impurity in PbTe. It is calculated without SOI using $2 \times 2 \times 2$ supercell. The corresponding carrier concentration is 4.4×10^{20}/cm^3.

The calculated band structures of K- and Na-doped PbTe are shown in Figs. 6(c), and 6(d), respectively, which agree well with earlier calculations by Hoang *et al.*[39] At the Γ point, which is the valence band maximum, both K/Na doping lead to a removal of the 8-fold degeneracy of pure PbTe. Removal of degeneracy is also observed at the second and third valence band maxima along Σ ($\langle 111 \rangle$) and Λ ($\langle 110 \rangle$) directions. In addition, the energy of VBM at Σ becomes lower than that at Λ for Na-doped PbTe. We find that K-doped compound shows less distortion in the band structure compared to the Na-doped one.

To see how changes in the band structure due to dopant impurities (K or Na) affect their thermopower, one has to calculate S using the calculated band structures with SOI for a very large number of **k**-points. This is too expensive computationally. We have therefore calculated S using CSC band structures in the absence of SOI. We note here that the band structure without SOI (Figure is not shown) also shows splitting of degenerate VBM along Γ to R direction (shown with arrows in the Figs. 6(c) and 6(d)) except the splitting of the two top-most bands along Λ, which is seen in the band structure with SOI. Furthermore the values of splitting of the degenerate bands at Γ are nearly the same (within a few meV) for both with and without SOI (0.07 eV for K doping and 0.12 eV for Na doping). We therefore believe that inclusion of SOI in the calculation of S will not change its value obtained in the absence of SOI significantly, particularly for the p-doped cases discussed in this paper.

The calculated S values are shown in Fig. 7, along with the RBA results. As expected, thermopower obtained with perturbed band structure is smaller than that obtained using RBA. For example, at 300 K we find $S = 110$ μV/K with RBA, compared to 95 μV/K calculated with perturbed band structure, a 12 % reduction.

Recently Singh has calculated S for doped PbTe using RBA, *i.e.* using the band structure of pure PbTe, including SOI.[40] The thermopower is $\sim$120 μV/K at 300 K for $n \geq 4 \times 10^{19}$/cm^3. However, experimental measurements of thermopower for K- and/or Na-doped systems give about 55 μV/K for the same concentration.[5] Theoretical values obtained within RBA are more than twice large. We think that a part of this discrepancy can be ascribed to RBA. The other source of discrepancy between experiment and theory is likely to be the constant τ approximation, which we will explore in the future.

IV. SUMMARY

The present study of impurities in the HfCoSb and PbTe compounds using QPA reveals that the band structure of the host system can be affected, sometimes strongly, by impurities. The degree of perturbation depends on the type of impurity. In HH HfCoSb, the effect of isovalent impurities (Hf$\rightarrow$Zr, Sb$\rightarrow$Bi) is usually small whereas for substitution at the Co site, which contribute to VBM and CBM, regions near VBM and CBM are perturbed strongly. The perturbation scales with the impurity concentration. We find that large changes in the band structure occur for dopant impurities and the least change occurs for Sb. In PbTe, K and Na doping strongly perturb the band structure, particularly by removing the degeneracy of the VBM. The removal of degeneracy of the VBM both in HfCoSb and PbTe reduces S by $\sim$20 % or more from its values calculated in RBA, suggesting that RBA usually overestimates $\mid S \mid$ and the power factor, $S^2\sigma$.

ACKNOWLEDGMENTS

This work was supported by the Center for Revolutionary Materials for Solid State Energy Conversion, an Energy Frontier Research Center funded by the U.S. Department of Energy, Office of Science, Office of Basic Energy Sciences under Award

Number DE-SC0001054. This research used resources of the National Energy Research Scientic Computing Center, which is supported by the Ofce of Science of the US Department of Energy under Contract No. DE-AC02-05CH11231.

[1] G. A. Slack, in *Proceedings of Thermoelectric Materials-New Directions and Approaches*, Pittsburgh, PA, 1997, edited by T. M. Tritt, M. G. Kanatzidis, H. B. Lyon, Jr., G. D. Mahan (Materials Research Society, Pittsburgh, PA, 1997), Vol. **478**, p. 47.
[2] G. J. Snyder and E. S. Toberer, Nat. Mater. **7**, 105 (2008).
[3] G. D. Mahan, J. O. Sofo, Proc. Natl. Acad. Sci. U.S.A. **93**, 7436 (1997).
[4] J. P. Heremans, V. Jovovic, E. S. Toberer, A. Saramat, K. Kurosaki, A. Charoenphakdee, S. Yamanaka, G. J. Snyder, Science **321**, 554 (2008).
[5] J. Androulakis, I. Todorov, D.-Y. Chung, S. Ballikaya, G. Wang, C. Uher, M. Kanatzidis, Phys. Rev. B **82**, 115209 (2010).
[6] W. Jeitschko, Metall. Trans. A **1**, 3159 (1970).
[7] F. G. Aliev, V. V. Moshchalkov, V. V. Kozyrkov, R. V. Skolozdra, and A. I. Belogorokhov, Z. Phys. B **75**, 167 (1989).
[8] F. G. Aliev, V. V. Kozyrkov, V. V. Moshchalkov, R. V. Skolozdra, and K. Durczewski, Z. Phys. B **80**, 353 (1990).
[9] S. Öğüt and K. M. Rabe, Phys. Rev. B **51**, 10443 (1995).
[10] P. Larson, S. D. Mahanti, S. Sportouch, and M. G. Kanatzidis, Phys. Rev. B **59**, 15660 (1999).
[11] B. R. K. Nanda and I. Dasgupta, J. Phys.: Condens. Matter **15**, 7307 (2003).
[12] C. Uher, S. Hu, J. Yang, G. P. Meisner, and D. T. Merelli, *Proceedings of 16th International Conference on Thermoelectrics* (IEEE, Piscataway, NJ, 1997) p. 485.
[13] G. Martinez, M. Schlüter, and M. L. Cohen, Phys. Rev. B *11*, 651 (1975) and references therein.
[14] C. Uher, J. Yang, S. Hu, D. T. Morelli, and G. P. Meisner, Phys. Rev. B **59**, 8615 (1999).
[15] H. Hohl, A. P. Ramirez, C. Goldmann, G. Ernst, B. Wolfing, and E. Bucher, J. Phys.: Condens. Matter **11**, 1697 (1999).
[16] K. Mastronardi, D. Young, C. C. Wang, P. Khalifah, R. J. Cava, and A. P. Ramirez, Appl. Phys. Lett. **74**, 1415 (1999).
[17] A. F. Ioffe, *Semiconductor Thermoelements and Thermoelectric Cooling* (Inforsearch, London, 1957).
[18] C. Wood, Rep. Prog. Phys. **51**, 459 (1988).
[19] D. M. Rowe, *CRC Handbook of Thermoelectrics* (CRC Press, Boca Raton, 1995).
[20] Y. I. Ravich, B. A. Efimova, and V. I. Tamarchenko, Phys. Status Solidi B **43**, 11 (1971).
[21] Y. I. Ravich, E. A. efimova, and I. A. Smirnov, *Semiconducting Lead Chalcogenides* (Plenum, New York, 1970), Vol. 5, p. 299.
[22] D. I. Bilc, S. D. Mahanti, and M. G. Kanatzidis, Phys. Rev. B **74**, 125202 (2006).
[23] S. Ahmad and S. D. Mahanti, Phys. Rev. B **81**, 165203 (2010).
[24] Bao-Ling Huang and Massoud Kaviany, Phys. Rev. B **77**, 125209 (2008).
[25] L. Chaput, P. Pécheur, J. Tobola, H. Scherrer, Phys. Rev. B **72**, 085126 (2005).
[26] A. Popescu and L. M. Woods, Appl. Phys. Lett. **97**, 052102 (2010).
[27] G. Kresse and D. Joubert, Phys. Rev. B 59, 1758 (1999); P. E. Blöchl, Phys. Rev. B **50**, 17953 (1994).
[28] G. Kresse and J. Hafner, Phys. Rev. B 47, 558 (1993); G. Kresse and J. Furthmüller, Comput. Mater. Sci. 6, 15 (1996); G. Kresse and J. Furthmüller, Phys. Rev. B 54, 11169 (1996); see website: http://cms.mpi.univie.ac.at/vasp/.
[29] J. P. Perdew, K. Burke, and M. Ernzerhof, Phys. Rev. Lett. **77**, 3865 (1996).
[30] P. Carrier and S.-H. Wei, Phys. Rev. B **70**, 035212 (2004).
[31] H. J. Monkhorst, J. D. Pack, Phys. Rev. B **13**, 5188 (1976).
[32] D. J. Singh, Semiconduc. Semimet. **70**, 125 (2001).
[33] G. K. H. Madsen, D. J. Singh, Comput. Phys. Commun. **175**, 67 (2006).
[34] G. K. H. Madsen, J. Am. Chem. Soc. **128**, 12140 (2006).
[35] T. J. Scheidemantel, C. Ambrosch-Draxl, T. Thonhauser, J. V. Badding, J. O. Sofo, Phys. Rev. B **68**, 125210 (2003).
[36] M. Lax, *Symmetry Principles in Solid State and Molecular Physics* (Wiley, New York, 2003).
[37] Mal-Soon Lee, Ferdinand P. Poudeu, and S. D. Mahanti, Phys. Rev. B **83**, 085204 (2011).
[38] Khang Hoang and S. D. Mahanti, Phys. Rev. B **78**, 085111 (2008).
[39] Khang Hoang, S. D. Mahanti, and M. G. Kanatzidis, Phys. Rev. B **81**, 115106 (2010).
[40] David J. Singh, Phys. Rev. B **81**, 195217 (2010).